CrossMark

Effect of 3d transition metal doping (Co, Ni and Cu) on structural, optical, morphological and dielectric properties of sol–gel assisted auto-combusted $Mg_{0.95}Mn_{0.05}O$ nanoparticles

Ishtihadah Islam[1] · Shakeel Ahmad Khandy[2] · M. Burhanuz Zaman[3] · Dinesh C. Gupta[2] · Aurangzeb Khurram Hafiz[1] · Azher Majid Siddiqui[1]

Abstract

We hereby report the synthesis of $Mg_{0.95}Mn_{0.05}O$ nanostructures using auto-combustion method. Effect of incorporation of different transition metal dopants (cobalt, nickel and copper) on structural, optical, morphological and dielectric properties of pristine $Mg_{0.95}Mn_{0.05}O$ is investigated. X-ray diffraction plots confirm the cubic crystal structure of these samples. The crystallite size is found to be 78.2, 67.02, 78.11 and 64 nm for pure, Co, Cu and Ni doped MgMnO, respectively. Raman analysis clearly envisages the purity of the presently synthesized samples. Optical transmission spectrum shows that samples are highly transparent in the UV–Visible region. In addition, the FTIR results established the presence of magnesium oxide in all samples. Dielectric characterization depicts a reasonable decrease in the dielectric constant ε' as function of improving frequency, which in turn confirms its dispersive nature.

1 Introduction

Tailoring of oxide material properties has been an interesting theme for material scientists to enhance the magnificent properties for technologically important applications. For the same, doping is a promising pathway and helps to meet the demands based on different electronic, optical and chemical applications of these materials [1, 2]. MgO is an important material with multiple applications like electronics, catalysis and optics, etc. [3]. Due to these interesting properties of magnesium oxide in bulk as well as in nano form, it has achieved a lot of attention from the researchers worldwide. In magnesium oxide, the presence of small impurity concentrations greatly affects its surface reactivity. Inconsistent distribution of dopant ions that exists at surfaces and interfaces, consequently changes surface energy of the host compound and structure sensitive properties of the material [4]. These oxide materials can be prepared by different synthesis methods such as solution combustion [5], co-precipitation [6], sol–gel [7], hydrothermal [8], solvothermal [9], microwave assisted Sol–gel [10], green synthesis [11]. Various transition metal dopants such as Cr [12], Fe [13] and Ni [14] have been reported so far in MgO resulting in change of some basic properties like the magnetic ones. Such doping of MgO changes its nature from diamagnetic to paramagnetic. Here we synthesize pristine $Mg_{0.94}Mn_{0.06}O$ and transition metal doped samples of $Mg_{0.94}Mn_{0.01}TM_{0.05}O$ (TM = Co, Ni, Cu) via sol–gel auto-combustion process. We approach this method as it allows easy doping of transition metals and is cost effective in nature. The prime idea behind this work is to study the effect of various transition metal dopants on the structural, optical, morphological and dielectric properties of MgO nanoparticles. Since, the enhancement of the desired properties has been achieved so far in the present investigations. Therefore, the detailed arguments are put forward in the Sect. 3. The corresponding characterization of synthesized samples has been achieved using X-ray diffraction (XRD; Bruker D8 Advance), UV–VIS–NIR spectrometer (Perkin Elmer lambda-950), FTIR spectrometer (Bruker Vertex-70), SEM (JEOL JSM 5600) and dielectric spectrometer.

✉ Shakeel Ahmad Khandy
shakeelkhandy11@gmail.com

[1] Department of Physics, Jamia Millia Islamia, New Delhi 110025, India

[2] Condensed Matter Theory Group, School of Studies in Physics, Jiwaji University, Gwalior, Madhya Pradesh 474011, India

[3] School of Studies in Physics, Jiwaji University, Gwalior, Madhya Pradesh 474011, India

2 Experimental details

All the chemicals were used as such without any further purification. Pure $Mg_{0.95}Mn_{0.05}O$ was synthesized using sol–gel auto-combustion method. Four different samples A, B, C and D were prepared containing pristine $Mg_{0.94}Mn_{0.06}O$ and transition metal doped samples of $Mg_{0.94}Mn_{0.01}TM_{0.05}O$ (TM = Co, Ni, Cu), respectively. The source materials selected for the synthesis were hydrated metal nitrates. Accordingly the metal nitrates were dissolved in 100 ml distilled water in appropriate molar ratios. After complete dissolution, citric acid was added to these solutions. Citric acid acted as a chelating agent and helps the reaction to proceed. Certain amount of ammonia was added drop-wise to maintain the pH of corresponding reaction mediums. All the four solutions were then allowed to stir on a magnetic stirrer for 6 h and at 80 °C. Auto-combustion of the corresponding gels resulted in black product formation. These burnt black powders were grinded for 3 h and vacuum annealed for 4 h at 600 °C. The samples thus synthesized were studied for structural, optical, morphological and dielectric properties.

3 Results and discussion

3.1 Structural properties

The structural and morphological investigations based on XRD results and SEM micrographs are discussed along with Raman spectrum. Figure 1a shows the XRD spectrum of synthesized samples. The XRD patterns of dried as-prepared and classified samples were obtained using an X-ray diffractometer with Cu Ka radiation (0.154 nm wavelength). The peak positions appearing at 2θ values of 37.02°, 42.95°, 62.31°, 74.69°, and 78.56° can be readily indexed as (111),

(200), (220), (311), and (222) crystal planes of the MgO, respectively. The main peaks are comparable to that of the standard powder diffraction spectrum of MgO (JCPDS card no. 78-0429) and those reported in the literature for cubic MgO having space group Fm-$3m$ [15]. Absence of any other peaks depicts the purity of the samples. The lattice parameter obtained from indexing is found to be almost constant (0.42 nm) for all the transition element doped samples. All samples have preferred orientation along (200) plane. The crystallite size is calculated for the main peak (200) using the Scherrer's formula [16]:

$$D = \frac{0.9\lambda}{\cos\theta}$$

where, λ is the X-ray wavelength used, β is the full width of the diffraction line at half its maximum intensity, and θ is the Bragg angle. The crystallite size was found to be 78.2, 67.02, 78.11 and 64 nm for pure, Co, Cu and Ni doped MgMnO, respectively.

Figure 1b represents the room temperature Raman spectra of $Mg_{0.95}Mn_{0.01}TM_{0.04}O$ (TM = Co, Ni and Cu) metal oxide nano particles within the range of 50 to 800 cm^{-1}. Raman analysis is carried out to check the purity of samples synthesized, as it takes into consideration the vibrational modes. The spectrum represents four optical phonon modes at ~381, 440, 474, 613 cm^{-1}. The peak values obtained at about 440 and at 613 cm^{-1} are assigned to low and high frequency E_2 mode of MgMnO lattice respectively, at 381 cm^{-1} A_1 transverse optical (TO) phonon mode and at 474 cm^{-1} longitudinal optical (LO) phonon of A_1 mode [17]. On the other hand, the peak at 381 cm^{-1} is attributed to E_1 TO phonon mode of MgMnO sub-lattices. However, only one mode of vibration is observed in Ni doped $Mg_{0.95}Mn_{0.01}Ni_{0.04}O$. Modes of vibration in $Mg_{0.95}Mn_{0.05}Co_{0.05}O$ and $Mg_{0.95}Mn_{0.05}Cu_{0.05}O$ are very similar to those of parent $Mg_{0.95}Mn_{0.05}O$. The obtained phonon modes are the indicative of high quality

Fig. 1 a XRD and b Raman spectrum of $Mg_{0.95}Mn_{0.01}TM_{0.04}O$ (TM = Co, Ni and Cu) metal oxide nano particles
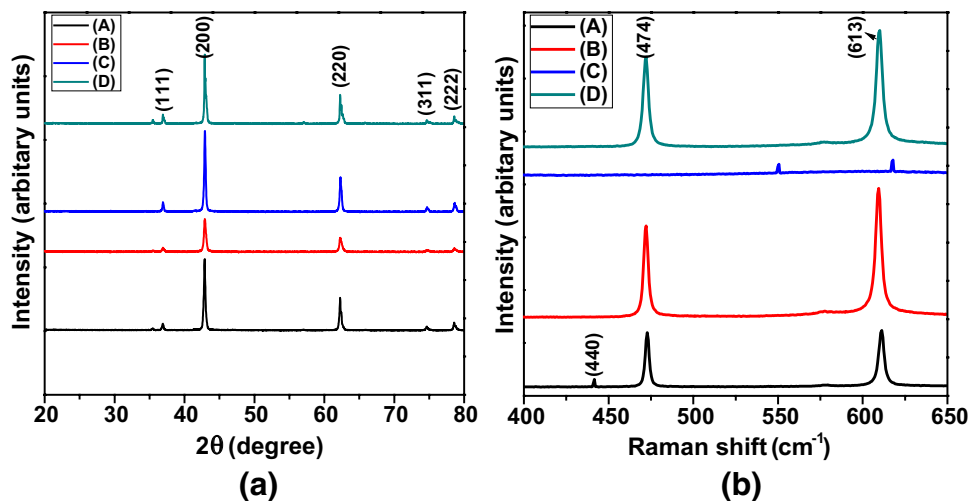
Cubic crystal structure of MgMnO nano-particles which is in agreement with XRD results.

Figure 2 represents the SEM micrographs of corresponding samples. These micrographs reveal a systematic evaluation of the morphology of synthesized crystalline samples. For all MgMnO samples, single-phase primary particles, nearly of spherical shaped nanocrystallites were observed. From the SEM micrograph it is clear that as synthesized

samples display the aggregation of smaller nanoparticles. The particle size seems to increase monotonously as we go from Co to Cu doping.

3.2 Optical properties

Figure 3a represents the transmission spectrum of $Mg_{0.95}Mn_{0.01}TM_{0.04}O$ (TM = Co, Ni and Cu) metal oxide

Fig. 2 SEM micrograph of $Mg_{0.95}Mn_{0.01}TM_{0.04}O$ (TM = Co, Ni, Cu) samples respectively
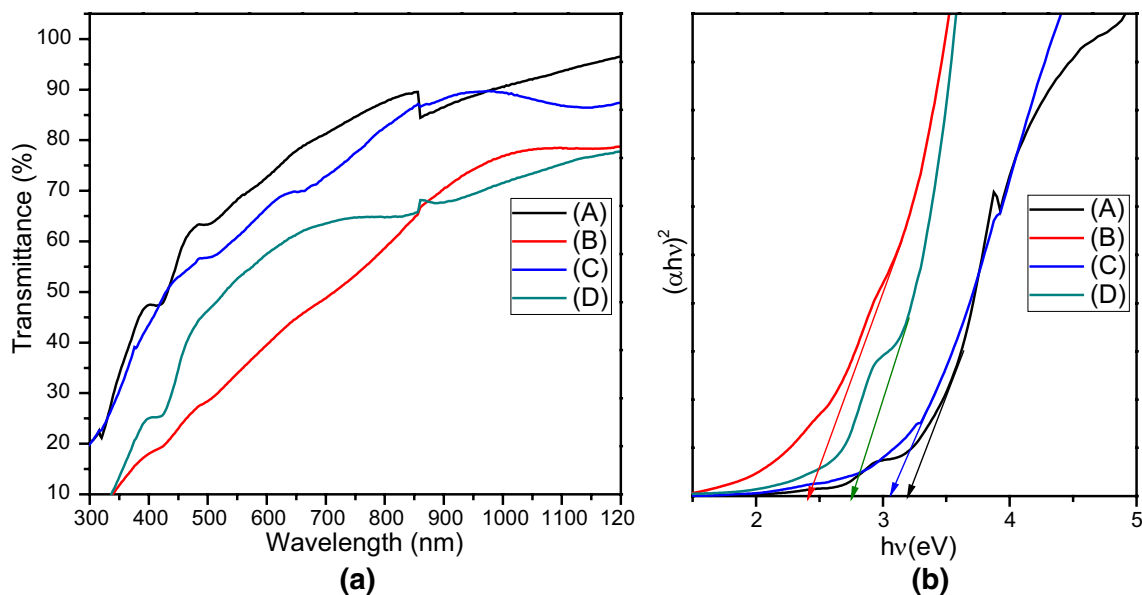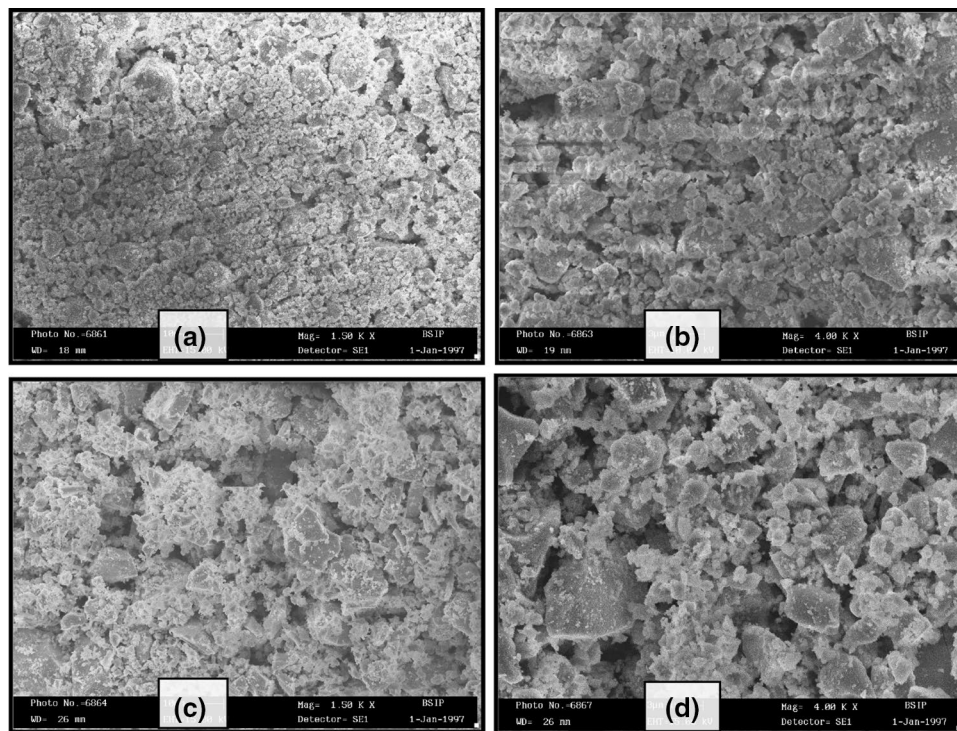
Fig. 3 **a** Transmission spectrum and **b** optical band gaps of $Mg_{0.95}Mn_{0.01}TM_{0.04}O$ (TM = Co, Ni and Cu) metal oxide nano particles

nano particles. All the samples show high transmittance over the entire visible region. From the transmission spectrum, optical band gap was calculated using Tauc plot [18]. Optical band gaps thus calculated for samples A, B, C and D were 3.2, 2.4, 3.1 and 2.7 eV, respectively. The decrease in band gap (E_g) in case of transition metal doping is attributed to the s–d and p–d interactions giving rise to band gap bowing and it has been theoretically explained using second-order perturbation theory [19].
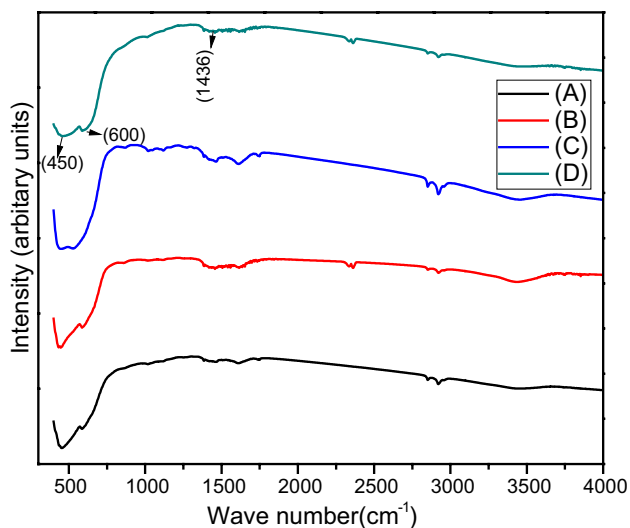

Fig. 4 FTIR spectrum of $Mg_{0.95}Mn_{0.01}TM_{0.04}O$ (TM = Co, Ni and Cu) metal oxide nano particles

Figure 4 represents the Fourier transform infrared (FTIR) spectrum of the synthesized sample pellets. FTIR spectroscopy is a powerful tool for identifying types of chemical bonds in a molecule by producing an infrared absorption spectrum that is like a molecular fingerprint. The spectrum clearly shows the broad band within 450–600 cm^{-1} which is associated with the special vibration of magnesium oxide [20]. The band at 1436 cm^{-1} corresponds to C–H bending [21]. The FT-IR spectrum of $Mg_{0.95}Mn_{0.01}TM_{0.04}O$ represents the combined bands of MnO–MgO oxides.

3.3 Dielectric properties

Figure 5a illustrates the frequency dependence of the dielectric constant (ε') for $Mg_{0.95}Mn_{0.01}TM_{0.04}O$ (TM = Co, Ni and Cu) metal oxide nanoparticles at room temperature. The graph depicts that dielectric constant ε' decreases as function of improving frequency from 1 Hz to 1 MHz confirming its dispersive nature [22]. The large values of dielectric constants at lower frequency (~100 Hz) are measured as 127.7, 9.32, 12.73, and 19.0 for $Mg_{0.95}Mn_{0.01}TM_{0.04}O$ (TM = Co, Ni and Cu) metal oxide nano particles respectively. The high values of ε' in case of $Mg_{0.95}Mn_{0.01}Co_{0.04}O$ might be due to grain boundary assisted polarization process. The dielectric constant in $Mg_{0.95}Mn_{0.01}TM_{0.04}O$ (TM = Co, Ni and Cu) metal oxide nano particles is less than those of $Co–Zn–Fe_2O_4$ and $Ni_{0.5}Zn_{0.5}Fe_2O_4$ [22]. It is observed that the permittivity at lower frequencies decreases rapidly and at higher frequencies this decrease is quite slow. The Co doped
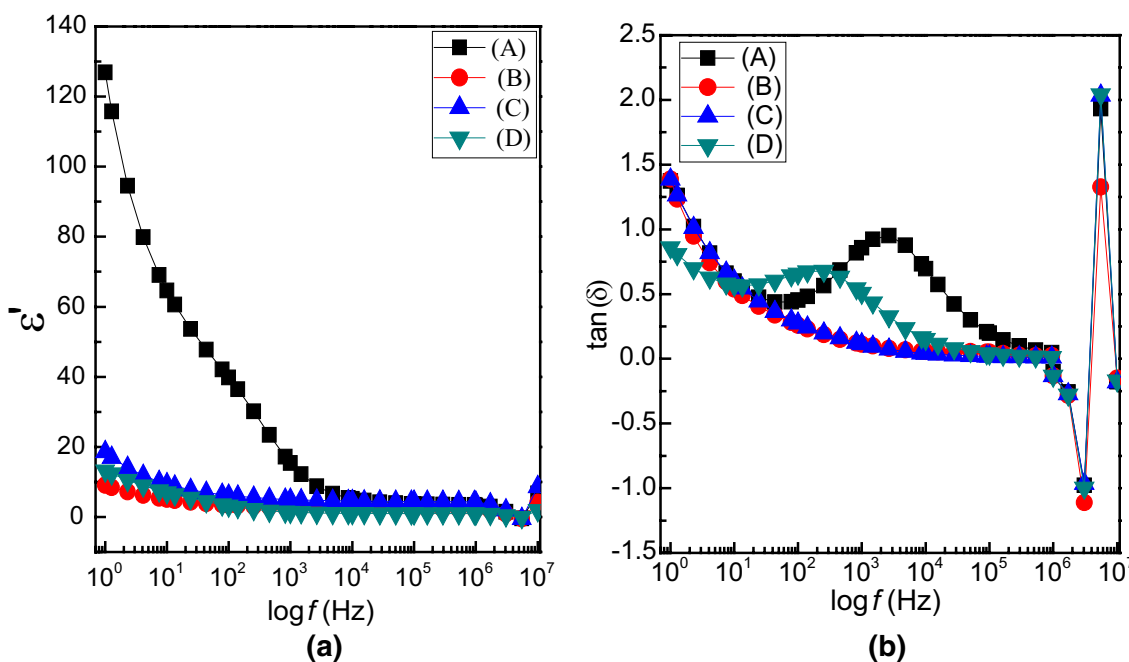
Fig. 5 **a** Variation of dielectric constant and **b** dielectric losses with frequency of $Mg_{0.95}Mn_{0.01}TM_{0.04}O$ (TM = Co, Ni and Cu) at room temperature

ferrites showed similar dispersive results earlier [22]. The frequency dependent dispersive nature of ε' is an indicative of space charge effect [23]. This decrease in dielectric constant ε' with frequency for transition metal doped MgO nano sized materials can be explained using the Koops theory [22], considering the dielectric structure as an inhomogeneous medium of two layers of the Maxwell–Wagner type [23].

Figure 5b shows the plot representing dielectric loss (tan δ) with frequency. The decrease in tan δ takes place when the jumping rate of charge carriers lags behind the alternating electric field beyond a certain critical frequency. However all the transition elements doped $Mg_{0.95}Mn_{0.01}TM_{0.04}O$ shows a shoulder like behavior in the range of 10^2–10^4 Hz.

4 Conclusion

We have adopted a very cheap and facile synthesis route *i.e*. sol–gel auto-combustion method for fabricating metal oxide nano-particles $Mg_{0.95}Mn_{0.01}TM_{0.04}O$ (TM = Co, Ni and Cu). XRD patterns confirm cubic structure of samples with crystallite sizes equal to 78.2, 67.02, 78.11 and 64 nm for pure, Co, Cu and Ni doped MgMnO, respectively. From the Raman analysis we got phonon modes depicting high quality cubic crystal structure of MgMnO nano-particles. SEM micrograph displayed the aggregation of smaller nanoparticles. The particle size seemed to increases monotonously as we go from Co to Cu doping. Addition of transition metal doping resulted decrease in optical band gap. The space charge effect is designated by the frequency dependent dispersive nature of ε', which can be explained using the Koops theory for nano materials. The dielectric permittivity decreases rapidly at lower frequencies and a slow decrease is observed at higher frequencies.

References

1. E.W. McFarland, H. Metiu, Catalysis by doped oxides. Chem. Rev. **113**, 4391–4427 (2013)
2. N. Nilius, H.-J. Freund, Activating nonreducible oxides via doping. Acc. Chem. Res. **48**, 1532–1539 (2015)
3. M.H. Rummeli, C. Kramberger, A. Gruneis, P. Ayala, T. Gemming, B. Buchner et al., On the graphitization nature of oxides for the formation of carbon nanostructures. Chem. Mater. **19**, 4105–4107 (2007)
4. W.D. Kingery, *Introduction to Ceramics*, (Wiley, New York, 1960), pp. 193, 408, 682
5. J. Bai, F. Meng, C. Wei, Y. Zhao, H. Tan, J. Liu, Solution combustion synthesis and characteristics of nanoscale MgO powders. Ceram. Silik. **55**(1), 20–25 (2011)
6. B. Vatsha, P. Tetyana, P.M. Shumbula, J.C. Ngila, L.M. Sikhwivhil, R.M. Moutloali, Effects of precipitation temperature on nanoparticle surface area and antibacterial behaviour of Mg(OH)$_2$ and MgO nanoparticles. J. Biomater. Nanobiotechnol. **4**, 365–373 (2013)
7. P. Tamilselvi, A. Yelilarasi, M. Hema, R. Anbarasan, Synthesis of hierarchical structured MgO by Sol–Gel method. Nano Bull. **2**(1), 130106 (2013)
8. H. Hayashi, Y. Hakuta, Hydrothermal synthesis of metal oxide nanoparticles in supercritical water. Materials **3**, 3794–3817 (2010)
9. Y. Hou, J. Yu, S. Gao, Solvothermal reduction synthesis and characterization of superparamagnetic magnetite nanoparticles. J. Mater. Chem **13**, 1983–1987 (2003)
10. H. Mirzaei, A. Davoodnia, Microwave assisted Sol-Gel synthesis of MgO nanoparticles and their catalytic activity in the synthesis of Hantzsch 1,4-dihydropyridines." Chin. J. Catal. **33**, 1502–1507 (2012)
11. A.B. Patil, B.M. Bhanage, Novel and green approach for the nano crystalline magnesium oxide synthesis and its catalytic performance in Claisen–Schmidt condensation. Catal. Commun. **36**, 79–83 (2013)
12. F. Stavale, N. Nilius, H.-J. Freund, New J. Phys. **14**, 033006 (2012)
13. A. Shalimov, K. Potzger, D. Geiger, H. Lichte, G. Talut, A. Misiuk, H. Reuther, F. Stromberg, S. Zhou, C. Baehtz, J. Fassbender, J. App. Phys. **105**, 064906, (2009)
14. S. Ramachandran, J. Narayan, J.T. Prater, Appl. Phys. Lett. **90**(13), 222505 (2007)
15. R. Wahab, S.G. Ansari, M.A. Dar, Y.S. Kim, H.S. Shin, Mater. Sci. Forum. **558–559**, 983–986 (2007)
16. T. Chandel, J. Singh, P. Rajaram, AIP Conf. Proc. **1675**, 0200321–0200324 (2015)
17. M.A. Dar, P. Narwaria, S. Barfa, D. Varshney, AIP Conf. Proc. **1832**, 050052, (2017)
18. U. Verma, V. Thakur, P. Rajaram, A.K. Shrivastava, Electron. Mater. Lett. **11**(1), 46–54 (2015)
19. R.B. Bylsma, W.M. Becker, J. Kossut, U. Debska, Dependence of energy gap on x and T in Zn$_{1-x}$ Mn$_x$ Se: the role of exchange interaction. Phys. Rev. B **33**, 8207–8215 (1986)
20. J. Wu, H. Yan, X. Zhang, L. Wei, X. Liu, B. Xu, J. Colloid Interface Sci. **324**, 167–171 (2008)
21. K.C. Barick, S. Sing, M. Aslam, D. Bahadur, Microporous Mesoporous Mater. **134**, 195–202 (2010)
22. D. Varshney, S. Dwivedi, Mater. Res. Express **2**, 106102 (2015)
23. S. Demirezen, A. Kaya, S.A. Yeriskin, M. Balbasi, I. Uslu, Results Phys. **6**, 180–185 (2016)